reviewer noted that 18C6 has six oxygen atoms for coordinating the Li^+, whereas triglyme has only four oxygen atoms. [In our Introduction we pointed out that 12C4, the cyclic analogue of triglyme, added to $LiAsF_6$ in DMC precipitates, thus necessitating our use of 18C6.] In response to this criticism we have obtained the mid-infrared spectra of 0.10 M $LiAsF_6$ + 0.10 M tetraglyme and of 0.10 M $LiAsF_6$ + 0.10 M 15C5 in DMC shown in parts A and B of Figure 8, respectively. The spectral envelope in the 740-660-cm^{-1} spectral region corresponding to the $\bar{\nu}_3$ mode of AsF_6^- can be described by the sum of three Gaussian-Lorentzian product functions. The satellite band at approximately 717 cm^{-1} has a smaller absorbance, $A°_{717}$, for $LiAsF_6$ + tetraglyme (Figure 8A) than for $LiAsF_6$ + triglyme (Figure 3), indicating that tetraglyme, $CH_3O(CH_2CH_2O)_3CH_3$, with five coordinating oxygen atoms coordinates Li^+ more effectively than does triglyme thus segregating the Li^+ ion from contact with AsF_6^-. Similar comparisons of the amplitudes of the ~717-cm^{-1} bands can be made for $LiAsF_6$ in DMC solutions of 15C5 (Figure 8B) versus 18C6 (figure 4B) and 18C6 (Figure 4B) versus tetraglyme (Figure 8A). With the number of oxygen atoms of a ligand in parentheses, the order of decreasing effectiveness in complexing Li^+ ion deduced from these infrared spectra is

15C5 (5) > 18C6 (6) > tetraglyme (5) > triglyme (4)

It follows that the cyclic nature of an ethereal ligand is a more important factor in determining its effectiveness as a ligand for Li^+ than the number of oxygen atoms, at least for these ligands in DMC.

A second reviewer pointed out another possible interpretation of our dielectric microwave relaxation data. Percolation theory[11] predicts that the "renewal time" (i.e., the time required for the polymer chains to rearrange themselves thus offering a free volume of translation to the ions) is the determining factor for ionic mobility and ionic molecular dynamics. It is thus important to ascertain whether a dielectric relaxation of triglyme in DMC exists in the same triglyme concentration range and frequency range as the relaxation found for $LiAsF_6$ + triglyme in DMC at 25 °C. Figure 9 clearly shows that for 0.15 M triglyme in DMC at 25 °C no relaxation exists at frequencies lower than that common to the DMC solvent. Thus, in this concentration range, it appears that we are still in the realm of single ion coordination chemistry as far as the polyether chains and ionic dynamics are concerned and not in the range of the cooperative phenomena envisaged by free volume[12] and percolation theories.[11] These latter views might, however, become relevant at much higher polyether concentrations, most notably in pure polyether solvents as well as in solid-state polymers to which one of these theories[11] specifically refers.

Registry No. $LiTG^+AsF_6^-$, 130246-80-9.

(11) Druger, S. D.; Ratner, M. A.; Nitzan, A. *Solid State Ionics* **1983**, *9-10*, 115. Druger, S. D.; Nitzan, A.; Ratner, M. A. *J. Chem. Phys.* **1983**, *79*, 3133. Druger, S. D.; Ratner, M. A.; Nitzan, A. *Phys. Rev. B: Condens. Matter* **1985**, *31*, 3939. Ratner, M. A. In *Polymer Electrolyte Reviews 1*; McGallum, J. R., Vincent, C. A., Eds.; Elsevier Applied Science: London, 1987.

(12) Cohen, M. H.; Turnbull, D. *J. Chem. Phys.* **1959**, *31*, 1164. Adam, G.; Gibbs, J. H. *J. Chem. Phys.* **1965**, *43*, 139.

Evidence That the Effects of Synthetic Amphiphile Vesicles on Reaction Rates Depend on Vesicle Size

Maria K. Kawamuro, Hernan Chaimovich, Elsa B. Abuin,† E. A. Lissi,† and Iolanda M. Cuccovia*

Departamento de Bioquimica, Instituto de Quimica da Universidade de Sao Paulo, Sao Paulo, Brazil
(Received: May 4, 1990)

Small and large vesicles were prepared with dioctadecyldimethylammonium chloride and bromide. The hydrodynamic radius of the small vesicles ranges from 11 to 30 nm, while that of the large vesicles is ca. 140 nm. Both small and large vesicles increased the rate of alkaline hydrolysis and thiolysis (heptyl mercaptan, HM) of *p*-nitrophenyl octanoate (NPO). The rate/amphiphile patterns were different and the small vesicles were 2-5-fold more effective as catalysts. From the quantitative analysis of the kinetic results, using a pseudophase model with ion exchange, we concluded that the size dependence is due to differences in ion dissociation, substrate binding constants, and intrinsic reactivities. The effect of vesicle size on substrate distribution was confirmed by measuring binding constants with a fluorescence quenching method. These data show that the rate differences arise mainly from a variation in the capacity of the bilayer to solubilize substrates and dissociate counterions. This work also shows that even small differences in bilayer packing, with no changes in medium or aggregate composition, can modulate the rate of supramolecular-modified chemical reactions.

Introduction

Amphiphile aggregates such as micelles, vesicles, microemulsions, and liquid-crystalline phases modify the rates and/or the mechanisms of a variety of reactions.[1] The aggregate structure, as well as the composition of the reaction medium, can lead to modulation of reaction rates by factors reaching several million fold.[1-3] Subtle differences in aggregate structure can sometimes produce significant effects. Thus, the photochemical isomerization of merocyanine changes abruptly when (liquid crystalline) potassium laurate passes from cylindric (N_c) to disklike (N_L) or micellar (L) phases.[4] Similar effects were observed for the bromination of *trans*-stilbene in the N_c to N_L transition in sodium decyl sulfate/water/1-decanol.[5] The same reaction exhibits structure-dependent changes in sodium dodecyl sulfate (SDS) micelles, dihexadecyl phosphate and dipalmitoylphosphatidylcholine vesicles.[6] Stereoselectivity, in the peptide-catalyzed

† Visiting Professor, Departamento de Quimica, Facultad de Ciencias, Universidad de Santiago de Chile, Santiago, Chile.

* To whom correspondence should be addressed at Departamento de Bioquimica, Instituto de Quimica, Universidade de Sao Paulo, Caixa Postal 20780, Sao Paulo, SP CEP 01498 Brazil

(1) Fendler, J. H. *Membrane Mimetic Chemistry*; Wiley: New York, 1982.

(2) Chaimovich, H.; Bonilha, J. B. S.; Zanette, D.; Cuccovia, I. M. In *Surfactants in Solutions*; Mittal, K. L., Lindman, B., Eds.; Plenum Press: New York, 1984; Vol. 2, p 1121.

(3) Kunitake, T.; Okahata, Y.; Ando, R.; Shinkai, S.; Hirakawa, S. *J. Am. Chem. Soc.* **1980**, *102*, 7877.

(4) Ramesh, V.; Labes, M. M. *J. Am. Chem. Soc.* **1987**, *109*, 3228.

(5) Ramesh, V.; Labes, M. M. *J. Am. Chem. Soc.* **1986**, *108*, 4643.

0022-3654/91/2095-1458$02.50/0

TABLE I: Alkaline Hydrolysis of *p*-Nitrophenyl Octanoate[a]

amphiphile (method, pH)	α[b]	D_h,[c] Å	$10^{-3}K_s$,[d] M^{-1}	k_ψ^{max}/k_ψ^{oe} ([C], mM)	$k_{2m}/k_2°$[f]
DODAC (EtOH, 9.47)	0.23	220	5.0	61 (0.50)	0.32
DODAC (sonic, 9.47)	0.21	520	5.2	59 (0.40)	0.20
DODAC ($CHCl_3$, 9.41)	0.044	2850	1.7	33 (1.00)	0.17
DODAB (sonic, 9.30)	0.13	650	18.0	42 (0.20)	0.15
DODAB ($CHCl_3$, 9.20)	0.043	2750	1.2	28 (1.3)	0.21

[a] Borate buffer (0.01 M), parameters used (see text) were $K_{OH/Br} = 0.08$, $K_{OH/Cl} = 0.16$, $K_{OH/borate} = 2.25$, $k_2° = 9.69\ M^{-1}\ s^{-1}$, $\bar{V} = 0.58$ (DODAC), 0.62 (DODAB) (L/mol). [b] Degree of ion dissociation.[17] [c] Hydrodynamic diameter.[17] [d] NPO–vesicle binding constant (see text). [e] Ratio of the maximum observed rate constant/rate constant in the absence of amphiphile at the same pH. [f] Ratio of vesicular/aqueous-phase second-order rate constants.

hydrolysis of a hydrophobic ester, is dramatically affected by the size of aggregates composed of hexadecyltrimethylammonium and ditetradecyldimethylammonium bromide.[7] Differences in the local polarity of the reaction sites in the aggregates are a possible source of the structure-dependent rate modulation.[4] Substrate distribution, localization, orientation, and local order can also be determining factors for the rate and reaction mechanism differences observed in the distinct aggregates.[1-7]

The structure–function relationships involved in rate (or mechanism) control by the variation of the structure of the aggregate are far from clear. The physical properties of bilayers depend on headgroup packing, which in turn is a function of the aggregate diameter.[8] Controlled variation of the vesicle diameter allows structural changes of the bilayer without changes in the molecular structure of the monomer and/or medium composition.

Here we studied the effect of vesicle size on the alkaline hydrolysis and thiolysis of *p*-nitrophenyl octanoate (Scheme I).

SCHEME I

$$O_2NPhOCOR + OH^- \rightarrow O_2NPhO^- + RCO_2^- + H^+ \quad (I)$$

$$O_2NPhOCOR + R'S^- \rightarrow O_2NPhO^- + RCOSR' \quad (II)$$

$$R = R' = C_7H_{15}$$

Vesicles of dioctadecyldimethylammonium chloride (DODAC) and bromide (DODAB), of diameters ranging from 200 to 3000 Å, were obtained by using different preparation methods,[9] and their effects on the rate of both reactions were determined. The kinetic data were analyzed quantitatively by using the pseudophase model with ion exchange (PPIE).[2,10,11] The rate changes were due mainly to size-dependent differences in the substrate-vesicle binding constants, variations in surface ion dissociation, and differences in intrinsic reactivity.

Materials and Methods

p-Nitrophenyl octanoate (NPO, kindly provided by Prof. O. A. El Seoud from this Institute) and *n*-heptyl mercaptan (HM, Aldrich) were used without purification. Stock solutions of NPO and HM were prepared in CH_3CN. Dioctadecyldimethylammonium chloride (DODAC, Herga Ind. Chim., Brazil) was purified as described.[11] Dioctadecyldimethylammonium bromide (DODAB, Eastman Kodak) was recrystallized from methanol/acetone (1:3 v/v).

Spectra were obtained with a Beckman spectrophotometer (M-25 or DU-7) at 30.0 ± 0.1 °C. HM concentration was determined by titration.[12] The concentrations of DODAC and DODAB were determined by monomer titration.[13] Monomer concentration of the chloroform-injected vesicles cannot be directly obtained by using our previously described procedure[13] (applicable to sonicated and ethanol-injected vesicles) since chloroform-injected vesicles were not totally destroyed by addition of Brij-35 even upon heating. We found that dilution of these vesicles with ethanol (50%, v/v) before the addition to orange-G gave excellent results. Probably ethanol addition led to destruction of the bilayer, solubilization of the DODAC (or DODAB) monomers and thus quantitative complexation with the dye. The rate of hydrolysis or thiolysis of NPO was followed at 405 (pH > 7) or 330 (pH < 7) nm, respectively. Apparent first-order rate constants (k_ψ), obtained from plots that were linear for (at least) 4 half-lives, are the average of three different experiments with deviations no greater than 5%.

Sonicated vesicles were prepared by treating a 0.01 M suspension of the amphiphile for 1 h at 50 °C in a Branson (M5X-10) bath sonicator. The preparation of ethanol-[1] and chloroform-injected[14] vesicles has been described. Vesicles were prepared in the presence of the buffers indicated in the Results section.

The apparent pK_a ($pK_{ap} = \log(1/K_{ap})$) of HM in the presence of vesicles was measured by determining the absorbance of the mercaptide ion at 240 nm by using the following relationship:[11]

$$pK_{ap} = pH - \log \frac{A_\psi - A_{HM}}{A_M - A_\psi} \quad (1)$$

A_ψ is the absorbance of the HM solution measured at a pH in the vicinity of the pK_a (between 9 and 10), A_{HM} the absorbance of the protonated HM (determined in 0.005 M HCl, pH 2.3), and A_M the absorbance of the mercaptide ion (determined at pH 12). The values of A_M and A_{HM} did not change upon addition of vesicles. pK_{ap} was determined at a single pH, and the absorbance measured as a function of added vesicles at constant [HM].

The kinetic results were fitted to the PPIE model (see Results) by using one or two adjustable parameters. The input data consisted of k_ψ/[amphiphile] data pairs, and the program allowed, after introduction of the proper equations and fixed parameter values, a multiparametric fit of the data to the corresponding equations. A PC-XT-compatible computer was used for all calculations.

The binding constants of NPO and HM to DODAC vesicles were determined using a fluorescence quenching method previously described.[15] Pyrene (Aldrich) was purified by recrystallization from ethanol and incorporated after vesicle preparation. All spectra and emission intensities were registered in a Perkin-Elmer LS5 luminescence spectrometer at 27 °C. Samples were excited at 337 nm, and emissions measured at 400 nm. The pyrene/DODAC mole ratio was maintained below 10^{-4}. All experiments were done in air-equilibrated solutions. Small aliquots of stock solutions of NPO and HM in CH_3CN were added to previously prepared vesicles. The total added volume of CH_3CN never exceeded 1% (v/v) of the volume of the aqueous solution.

Results

The effects of sonicated and ethanol-injected DODAC vesicles on the rate of alkaline hydrolysis of NPO were similar: a sharp

(6) Mizutani, T.; Whitten, D. G. *J. Am. Chem. Soc.* **1985**, *107*, 3621.
(7) Ueoka, R.; Moss, R. A.; Swarup, S.; Matsumoto, Y.; Strauss, G.; Murakami, Y. *J. Am. Chem. Soc.* **1985**, *107*, 2185.
(8) Israelachvili, J. N. *Intermolecular and Surface Forces*; Academic Press: New York, 1985.
(9) Carmona-Ribeiro, A. M.; Yoshida, L. S.; Sesso, A.; Chaimovich, H. *J. Colloid Interface Sci.* **1984**, *100*, 433.
(10) Quina, F. H.; Chaimovich, H. *J. Phys. Chem.* **1979**, *83*, 1844.
(11) Cuccovia, I. M.; Quina, F. H.; Chaimovich, H. *Tetrahedron* **1982**, *28*, 917.
(12) Ellman, G. L. *Arch. Biochem. Biophys.* **1959**, *82*, 70.
(13) Stelmo, M.; Chaimovich, H.; Cuccovia, I. M. *J. Colloid Interface Sci.* **1987**, *117*, 200.
(14) Carmona-Ribeiro, A. M.; Chaimovich, H. *Biochim. Biophys. Acta* **1983**, *733*, 172.
(15) (a) Abuin, E. B.; Lissi, E. *J. Colloid Interface Sci.* **1983**, *95*, 198. (b) Abuin, E.; Lissi, E.; Aravena, D.; Zanocco, A.; Macuer, M. *J. Colloid Interface Sci.* **1988**, *122*, 201.

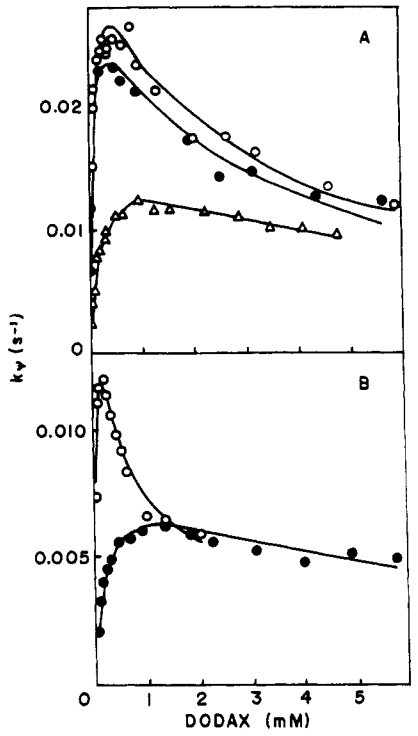

Figure 1. Effect of vesicles on the rate constant for alkaline hydrolysis of *p*-nitrophenyl octanoate. Borate buffer 0.01 M; [NPO] = 1×10^{-5} M. (A) DODAC (pH = 9.45): (○) ethanolic; (●) sonicated: (△) large vesicles. (B) DODAB: (○) sonicated (pH = 9.3); (●) large vesicles (pH = 9.2).

increase of k_ψ followed by a plateau and a decrease at higher amphiphile concentrations (Figure 1A). This pattern is comparable to several observations of the effect of sonicated vesicles and micelles on bimolecular reactions.[1-3] The effect of chloroformic vesicles (large vesicles, Table I) was similar, but the maximum observed rate constant (k_ψ^{max}) was lower and the rate decrease less pronounced (Figure 1A). The ratio between k_ψ^{max} and the k_ψ obtained in the absence of added amphiphile at the same pH ($k_\psi°$) for large vesicles was approximately half that obtained with sonicated vesicles (Table I). The differences between the effects of sonicated (small, Table I) and large vesicles on the alkaline hydrolysis of NPO was independent of the nature of the counterion, a very similar phenomena being observed for DODAB (Figure 1B, Table I).

The results shown in Figure 1 were analyzed by using eq 2,[16]

$$k_\psi = \frac{[OH_f]\{(k_{2m}/\bar{V})K_s K_{OH/Y}(Y_b/Y_f) + k_2°\}}{1 + K_s C} \quad (2)$$

where k_{2m} and $k_2°$ (9.69 M^{-1} s^{-1})[16] are the second-order rate constants in the vesicle and in the aqueous phase, respectively. K_s and $K_{OH/Y}$ are the NPO–vesicle binding constant and the ion-exchange constant (OH^-/halide), respectively. $[OH_f]$ is the hydroxide ion concentration in the intervesicular aqueous phase, C the analytical concentration of amphiphile, and $\bar{V}$ the partial molar volume of the amphiphile. Y_b and Y_f, the analytical concentrations of bound and free vesicular counterions (Cl^- ion in the case of DODAC and Br^- ion with DODAB), were calculated by using eq 3 and 4, where α is the degree of ion dissociation of

$$Y_b = (1 - \alpha)C - [OH_b] - [B_b] \quad (3)$$

$$Y_f = \alpha C + [OH_b] + [B_b] \quad (4)$$

the vesicle and C the total concentration of the amphiphile (expressed as moles/liter of monomer).[2] $[B_b]$ and $[OH_b]$ are the concentrations of the anionic form of the buffer and OH^- ion bound to the vesicle, respectively.[16] The values of $K_{OH/Br}$, $K_{OH/Cl}$, and $K_{OH/borate}$ used to calculate $[OH_b]$ and $[B_b]$ were 0.08, 0.16, and 2.25, respectively.[2,10,16] The values of α were those determined previously[17] and are presented in Table I. We have assumed that α is identical in the external and internal surfaces. $\bar{V}$ was calculated by multiplying the partial specific volume determined for lecithin (0.9848 mL/g)[18] by the molecular weight of the amphiphiles.[18] The values of $\bar{V}$ were 0.58 and 0.62 L/mol for DODAC or DODAB, respectively. The computer fit (Materials and Methods) of the data presented in Figure 1 gave the values of K_s and k_{2m} presented in Table I. The (best fit) value for K_s of NPO in sonicated vesicles was significantly higher than that observed for the large vesicles of the same amphiphile. The $k_{2m}/k_2°$ ratio, a measure of the effect of the vesicles on intrinsic reactivity, was not particularly sensitive to vesicle size (Table I).

TABLE II: Binding Constants of *n*-Heptyl Mercaptan (K_{HM}) and *p*-Nitrophenyl Octanoate (K_s) to DODAC Vesicles[a]

vesicle prep method	K_{HM}	$10^{-3}K$, M^{-1}	
		K_s	K_s^b
$CHCl_3$ injection	0.5 ± 0.02	1.0 ± 0.1	2.8 ± 0.4
sonicated	1.2 ± 0.1	4.0 ± 0.2	3.9 ± 0.2
ethanol injection	2.8 ± 0.2	3.9 ± 0.2	5.5 ± 0.4

[a] Vesicles prepared in 0.002 M HCl; values are the averages of at least three independent experiments ± the standard deviation. Experiments were done with 0.5–5 mM DODAC.[15b] [b] NPO–vesicle binding constants measured in the presence of HM maintaining a constant value of 0.03 for the mole ratios of incorporated HM/DODAC.

In addition to the assumptions underlying the PPIE model, the use of this formalism in vesicular systems implies the use of a single k_{2m} (corresponding to intra- and extravesicular reaction)[19] and fast equilibration of NPO between the reaction sites. The assumption of a single rate constant is reasonable because we have shown previously that OH^- reactivity in the external and internal interfaces of large vesicles is comparable.[19] The rate of transmembrane equilibration of relatively low molecular weight hydrophobic compounds (such as NPO and HM) is fast compared with the time scale of the reactions described here.[20] Evidence for fast inner–outer equilibration was obtained demonstrating that the quenching of vesicle-incorporated pyrene by NPO was the same before and after a heating (50 °C)–cooling (27 °C) cycle (not shown). Thus, NPO was rapidly and uniformly distributed in this time scale when added externally, even below the phase transition temperature of the DODAC bilayer.[14,21]

The distributions of NPO and HM between vesicles and bulk solution were measured by using a method based on the analysis of the changes in fluorescence intensity of a vesicle-incorporated probe upon substrate addition.[15] The values of the NPO and HM binding constants (K_s) to DODAC vesicles, as well as the effect of HM incorporation in the vesicles on the K_s of NPO, obtained in 0.002 M HCl, are given in Table II. The values of K_s of NPO obtained by fluorescence are very similar to those calculated from the analysis of kinetic data (compare Tables I and II). As observed previously for the incorporation of alcohols,[15b] HM and NPO partitioned more effectively into smaller vesicles. Incorporation of HM, particularly in large vesicles, increased the K_s of NPO (Table II).

The association of HM to the vesicles was also evaluated determining the effect of the amphiphile on the apparent pK (pK_{ap}) of HM. The data shown in Figure 2 were obtained at different pH's to facilitate the spectrophotometric measurements. pK_{ap} decreased to a minimum upon vesicle addition (Figure 2). In all these experiments the absorbance at 240 nm (see methods) was

(16) Quina, F. H.; Politi, M. J.; Cuccovia, I. M.; Baumgarten, E.; Martins-Franchetti, S. M.; Chaimovich, H. *J. Phys. Chem.* **1980**, *84*, 361.

(17) Cuccovia, I. M.; Feitosa, E.; Chaimovich, H.; Sepulveda, L.; Reed, W. *J. Phys. Chem.* **1990**, *94*, 3722.

(18) Newman, J. C.; Huang, C. *Biochemistry* **1975**, *14*, 3363.

(19) Cuccovia, I. M.; Kawamuro, M. K.; Krutman, M. A. K.; Chaimovich, H. *J. Am. Chem. Soc.* **1989**, *111*, 365.

(20) Jain, M. J. *The Bimolecular Lipid Membrane: A System*; Van Nostrand Reinhold: New York, 1972.

(21) Cuccovia, I. M.; Chaimovich, H.; Lissi, E.; Abuin, E. *Langmuir* **1990**, *6*, 1601–1604.

TABLE III: Thiolysis of *p*-Nitrophenyl Octanoate by *n*-Heptyl Mercaptan[a]

amphiphile (method, pH)	$10^{-3}K_{HM}$,[b] M^{-1}	$K_{M/Y}$[c]	$10^{-3}K_s$,[b] M^{-1}	$k_\psi^{max}/k_\psi^\circ$, ([C], mM)	k_{2m}/k_2°
DODAC[d] (EtOH, 5.35)	3.5	127	12.5	3.4×10^6 (0.11)	28
DODAC[d] (sonic, 5.35)	2.0	102	7.0	3.6×10^6 (0.16)	38
DODAC[e] ($CHCl_3$, 7.17)	0.5	5.1	2.5	2.7×10^5 (0.48)	68
DODAB[f] (sonic, 6.46)	2.5	18.1	30 (18[j])	7.4×10^5 (0.10)	20 (19[j])
DODAB[f] ($CHCl_3$, 6.55)	0.6	5.3	10 (1.2[j])	1.3×10^5 (0.20)	11 (15[j])

[a] $K_{OH/Br}$ = 0.08, $K_{OH/acetate}$ = 1.14, k_2° = 30 M^{-1} s^{-1}, $\bar{V}$ = 0.58 (DODAC), 0.62 (DODAB) (L/mol). [b] Best-fit parameter (see text). [c] Mercaptide–halide ion-exchange constant. [d] Na acetate, 5 mM. [e] Tris-acetate, 6 mM. [f] Pyperazine–acetate, 6 mM. [j] Alternative values of K_s and k_{2m}/k_2° used in the simulation of the data presented in Figure 3B.

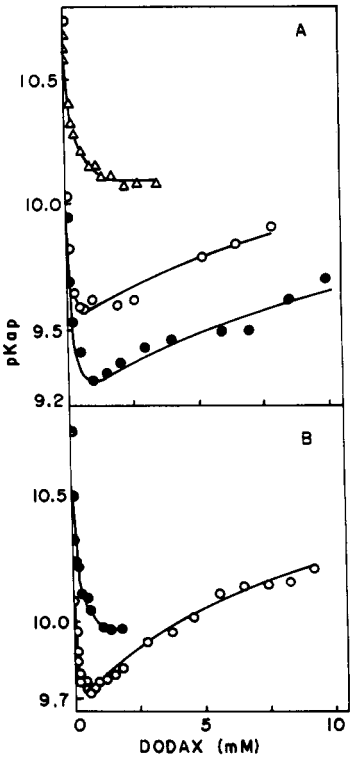

Figure 2. Effect of vesicles on the apparent pK_a of heptyl mercaptan. [HM] = (5–8) × 10^{-5} M. (A) DODAC: (○) ethanolic (Tris-acetate buffer, 0.05 M, pH = 9.02); (●) sonicated (Tris–acetate buffer, 0.05 M, pH = 9.2); (△) large vesicles (borate buffer, 0.01 M, pH = 10.14). (B) DODAB: (○) sonicated (borate buffer, 0.01 M, pH = 9.18); (●) large vesicles (borate buffer, 0.06 M, pH = 9.86).

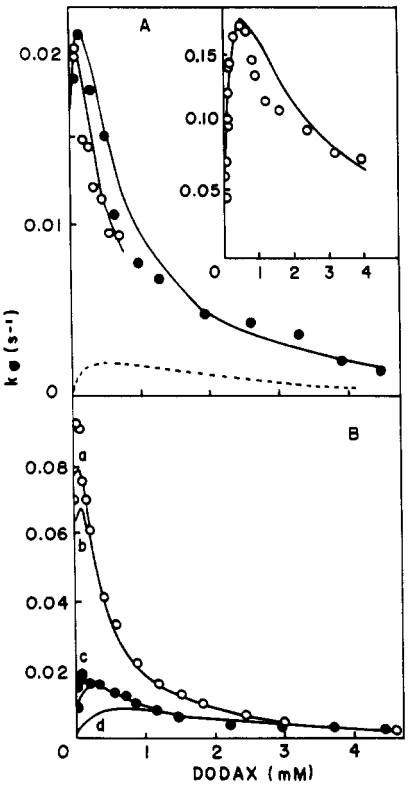

Figure 3. Effect of vesicles on the thiolysis of *p*-nitrophenyl octanoate by heptyl mercaptan. [NPO] = 5 × 10^{-6} M. (A) DODAC: (○) ethanolic (Tris–acetate buffer, 0.05 M, pH = 5.35, [HM] = 5 × 10^{-5} M); (●) sonicated (Na^+ acetate buffer, 0.05 M, pH = 5.35, [HM] = 5 × 10^{-5} M); (- - -) large vesicles, pH = 5.35, calculated (see text). Inset shows large vesicles (Tris–acetate buffer, 0.006 M, pH = 7.17, [HM] = 8.2 × 10^{-5} M). (B) DODAB: (○) sonicated (piperazine–acetate buffer, 0.006 M, pH = 6.46, [HM] = 8.18 × 10^{-5} M); (●) large vesicles (piperazine–acetate buffer, 0.0066 M, pH = 6.57, [HM] = 8.4 × 10^{-5} M). Lines were calculated (see text) by using the following values of K_s: sonicated 3.0 × 10^4 M^{-1} (a) and 1.8 × 10^4 M^{-1} (b); large vesicles 1.0 × 10^4 M^{-1} (c) and 1.2 × 10^3 M^{-1} (d).

measured by using a reference containing the same concentration of vesicles. With large vesicles the increase in light scattering at this wavelength prevented the use of higher amphiphile concentrations. Quantitative analysis of the variation of pK_{ap} (Materials and Methods) with amphiphile concentration was done with using eq 5,[10,16] where K_a is the acid dissociation constant of

$$K_{ap} = K_a \frac{1 + K_{M/Y}(Y_b/Y_f)}{1 + K_{HM}C} \quad (5)$$

HM in the aqueous phase (pK_a = 10.75),[2,22] K_{HM} the association constant of the protonated form of HM, and $K_{M/Y}$ the ion-exchange constant for the mercaptide/halide exchange. The calculated (best fit, see Materials and Methods) values of K_{HM} and $K_{M/Y}$ are presented in Table III. Both the $K_{M/Y}$'s and the K_{HM}'s obtained in small vesicles were significantly higher than those obtained in large vesicles both for DODAC and DODAB. The best fit values of K_{HM} were very similar with those obtained by fluorescence (compare Tables II and III).

Vesicles of DODAC and DODAB markedly increased the rate of thiolysis of NPO by HM (Figure 3). The ratio between k_ψ^{max} and the calculated rate constant for uncatalyzed thiolysis (k_ψ°) ($k_\psi^{max}/k_\psi^\circ$) reached 4 × 10^6-fold (Table III). The $k_\psi^{max}/k_\psi^\circ$ ratio was larger for small vesicles with both DODAC and DODAB (Table III). A significant difference in k_ψ^{max} between sonicated and large vesicles is evident upon inspection of Figure 3. With sonicated DODAC vesicles the reaction rate at pH 5.35 was significantly higher than that of HM oxidation (not shown). At the same pH, however, the rate of thiolysis in the presence of large vesicles was smaller and the rate of HM oxidation becomes significant (not shown). Thus, thiolysis with large DODAC vesicles was studied at pH 7.17 (Figure 3, inset). For comparative purposes we have included a calculation of thiolysis at pH 5.23 for large vesicles using the parameters obtained at pH 7.17 (Figure 3). Quantitative analysis of thiolysis was done using eq 6,[2,10] where

$$k_\psi = [HM_T]K_a\left[\frac{(k_{2m}/\bar{V})(K_sK_{M/Y})(Y_b/Y_f) + k_2^\circ}{(1 + K_{HM}C)([H_f] + K_{ap})(1 + K_sC)}\right] \quad (6)$$

$[HM_T]$ is the total concentration of HM, k_2° the second-order rate constant for thiolysis in aqueous solution (k_2° = 30 M^{-1} s^{-1}),[2,23]

(22) Yabroff, D. L. *Ind. Eng. Chem.* **1940**, *32*, 257.

k_{2m} the second-order rate constant in the vesicle, and $[H_f]$ the proton concentration in the aqueous solution (calculated from the measured pH). The values used for K_{HM} and $K_{M/Y}$ were those calculated from the analysis of pK_{ap} variation (see above). Curve fitting with the values of K_s previously calculated from the hydrolysis data (see above) was not possible, and K_s was used as an adjustable parameter, together with k_{2m}. The best fit value of K_s for DODAC was 2 times larger than that obtained from the hydrolysis data (compare Tables I and III). For DODAB we show the effect of K_s variation upon the shape of the k_ψ vs concentration profile (Figure 3B). The most discriminating region in our fitting procedure is that at low amphiphile concentration, where a large variation of k_ψ with [amphiphile] occurs and the molar ratio of HM/amphiphile was nearly 7 (Figure 3B). The differences between the values of K_s of NPO calculated in the thiolysis and hydrolysis reactions were clearly due to the effect of HM incorporated in the vesicle on the distribution constant of NPO, as demonstrated in Table II. The values of k_{2m}/k_2° are only slightly different, varying from 10 to 70 with different vesicle sizes and counterions (Table III). In all cases, the calculated reactivities in the vesicles were higher than those in aqueous solution.

Discussion

Single bilayer vesicles, ranging from 200 Å to several micrometers in diameter, can be obtained by using several preparation methods.[14,24,25] The size and the number of compartments of such vesicles have been determined by using a variety of physical techniques. In particular, DODAC and DODAB yield small (by sonication and ethanol injection)[17] and large (chloroform injection)[9,17] vesicles displaying a number of size-dependent properties. Small DODAC vesicles fuse upon addition of salt while large vesicles aggregate under the same conditions.[25] Differential osmometric behavior for both preparations has also been described.[14] The extent of ion dissociation from the outer surface (α) of small vesicles can be 10 times higher than that of large vesicles.[17] The capacity for solubilizing amphiphilic compounds is also affected by vesicle size.[15b] The measured binding constant of a series of alcohols is consistently lower for large vesicles, indicating that the bilayer has a lower capacity for accepting (at least) these compounds.[15b]

Qualitative differences in the effect of small and large vesicles upon the pK_{ap} of HM and on the rates of hydrolysis and thiolysis of *p*-nitrophenyl octanoate were evident upon inspection of the data (Figures 1–3). The apparent catalytic effect ($k_\psi^{max}/k_\psi^\circ$) for both reactions was higher in small vesicles. In the hydrolysis of NPO the difference in $k_\psi^{max}/k_\psi^\circ$ (small/large) in both DODAC and DODAB is ca. 2 (Table I). In the thiolysis reaction the apparent catalytic effect obtained with small vesicles is larger by a factor of 5 (DODAB) to 10 (DODAC, Table III).

Understanding the nature of the size-dependent kinetic effects requires dissection of the observed effect into its various components. In (the related) micellar systems separation of the role of individual rate-modifying factors was possibly only by using models for the quantitative analysis of observed rate data.[1] Several models for the quantitative analysis of micellar modified reactions have been put forward over the past decades.[1,10,26] The models—and the rationale for the analysis—varies. However, application of the models leads to the identification of the same factors as responsible for micellar effects on reaction. Intrinsic reactivity components, changes in the pK_a of dissociable nucleophiles, and (mainly) local concentration are the most important contributions to the observed effects. In selecting one particular model for the quantitative analysis of vesicle effects, i.e., PPIE, we are aware of the pitfalls in the use of this model.[26] Several reasons led us to use the PPIE model in this case. Apart from its simplicity, the number of uncertainties in the reaction sites probed by the systems described here demands the use of a tractable model. As shown in the Results, we have assumed that the system can be described by a single vesicular rate constant. The intrinsic reactivity of OH^- is comparable at both the inner and outer surfaces of large vesicles.[19] We have recently demonstrated, using the OH^- attack on 4-cyanopyridinium ions, that the reactivity of OH^- ion in the internal aqueous compartment of large vesicles is comparable to that in water.[27] Thus it is reasonable to use a single k_{2m} to analyze the vesicle data. Moreover, the outer area in small vesicles corresponds to about 70% of the total available reaction area, and thus it is to be expected that the major site of reaction occurs at the outer surface. Our choice of a value for the partial molar volume is also open for discussion. The definition of a reaction volume presupposes the exact knowledge of the reaction site(s). Even where the problem is simplified, as in the case of micelles, the exact definition of a reaction volume is debatable.[2,11,26] For comparative purposes our choice of $\bar{V}$ as the partial molar volume of the aggregated amphiphile is reasonable. One major unknown, however, is the ion dissociation at the internal surface. The best-fit values of k_{2m} and K_s were unaffected by values of α lower than 0.04. Thus, the best-fit values of the parameters obtained with large vesicles, which exhibit a low α, are little affected by our choice of α. On the other hand, the value of $K_{M/Y}$ varied by as much as a factor of 2 when the value of α of the small vesicles was decreased from 0.2 to 0. We have thus preferred to use a simple well-tested model for the sake of comparison, rather than trying to apply a more sophisticated framework in a system that is poorly understood.

Hydrolysis and thiolysis reactions in small sonicated vesicles have been analyzed quantitatively in a limited number of systems.[1] The excellent fit of the PPIE model to the present data, using some independently determined parameters, ensures that the pseudophase model can be applied to vesicles. Although the rate of OH^- attack is increased in the presence of vesicles, this kinetic effect arises from a concentration of the reagents in the vesicles rather than from a decrease in the activation energy required for the attack. As in other amphiphile-modified alkaline hydrolysis,[2] the k_{2m}/k_2° was less than one indicating an inhibition of 3–7-fold of the reaction in the vesicles (Table I). In CTAB micelles the k_{2m}/k_2° ratio is 0.3 for the same reaction.[2] The calculated values for k_{2m} for small and large vesicles were comparable. Thus the difference in the k_ψ vs [amphiphile] profiles arises mainly from differences in ion dissociation from—and substrate binding to—large and small vesicles.

Both heptyl mercaptan dissociation and NPO thiolysis in the presence of vesicles were well described by using the PPIE model. As in the case of hydrolysis the differential rate effects of small and large vesicles was clearly due to major differences in the association constants of the substrates and extent of ion dissociation from the surface(s). The differential effects of small and large vesicles on the pK_{ap} profiles of HM originate from variations in K_{HM} and $K_{H/Y}$. The fit of the data led to the finding that the protonated HM is less soluble in large vesicles and that Cl^- (or Br^-) ion is displaced less efficiently by mercaptide ion in the large vesicles. These results suggest a more impenetrable character of the large vesicles. Comparable results were obtained for the distribution of NPO using independent methods (Tables I–III).

Increasing evidence shows that the variations in headgroup packing, resulting from changes in vesicle size, cause differences in the association constants for both amphiphilic substrates and ions.[17,15b] In ester thiolysis the apparent catalytic effects of vesicles are larger than those obtained with micelles.[2] The $k_\psi^{max}/k_\psi^\circ$ ratios obtained with small vesicles were larger than those observed with large vesicles by a factor of 10 (DODAC) or 6 (DODAB). In all cases the k_{2m} are 10–60 times larger than k_2° while in CTAB micelles the k_{2m}/k_2° ratio is 1.0.[2] Changes in the structure of the supramolecular aggregate are effectively discriminated by using thiolysis as a test reaction. Vesicles efficiently increase mercaptide ion reactivity at the interface and the reactivity can be further

(23) Hupe, D. J.; Jencks, W. P. *J. Am. Chem. Soc.* **1977**, *99*, 451.
(24) Lasič, D. D. *J. Theor. Biol.* **1987**, *124*, 35.
(25) Carmona-Ribeiro, A. M.; Yoshida, L. S.; Chaimovich, H. *J. Phys. Chem.* **1985**, *89*, 2928.
(26) (a) Bacaloglu, R.; Bunton, C. A.; Ortega, F. *J. Phys. Chem.* **1989**, *93*, 1497. (b) Neves, M. F. S.; Zanette, D.; Quina, F. H.; Moretti, M. T.; Nome, F. *J. Phys. Chem.* **1989**, *93*, 1502.
(27) Cuccovia, I. M.; Chaimovich, H. *Bol. Soc. Chil. Quim.* **1990**, *35*, 39.

modulated by vesicle size by a factor of 2 (Table III). These findings suggest that for reactions that are more sensitive to medium composition the structure-dependent modulation can be even larger. The same amphiphile can modulate the reaction by a variety of different factors including subtle structural modifications. Structural changes due to monomer packing in vesicles of different diameters lead to differences in the characteristics of the interfacial reaction site. This additional reaction control mechanism, together with changing association constants and/or ion dissociation, can be of importance to fine tune reaction rates even in systems where the rate acceleration is of several million fold.

In conclusion we have demonstrated that the variation in vesicle size produces significant changes in the effect of these aggregates on reaction rates. The kinetic results were analyzed quantitatively, and the values of the substrate binding parameters were confirmed by using an independent, nonkinetic, method. These data show that the rate of differences arise mainly from a variation in the capacity of the bilayer to solubilize substrate. Moreover we have demonstrated that the solubilization of one substrate, even at low substrate/amphiphile ratio, can affect the binding of a second substrate, specially in large, planar-like bilayers.

Acknowledgment. This work was partially supported by grants from FAPESP, FINEP, CNPq, TWAS, CAPES, and BID-USP to H.C. and I.M.C. E.B.A. and E.A.L. thank the BID-USP project for Visiting Professor Fellowships. We are grateful to Dr. M. Armelin for her critical reading of the manuscript.

Registry No. NPO, 1956-10-1; HM, 1639-09-4; DODAC, 107-64-2; DODAB, 3700-67-2.

Temperature Dependence of Emulsion Morphologies and the Dispersion Morphology Diagram

Duane H. Smith,*,† G. C. Covatch, and Kyung-Hee Lim‡

U.S. Department of Energy, Morgantown Energy Technology Center, Morgantown, West Virginia 26507-0880
(Received: May 14, 1990)

The recently constructed "dispersion morphology diagram" predicts that for amphiphile/oil/water systems there exists a range of concentrations within which only OL/AQ ("oil-in-water") emulsions form and another range of concentrations for which the emulsion morphology is always AQ/OL ("water-in-oil"), regardless of whether the temperature is below the lower critical end-point temperature, above the upper critical end point, or between these two temperatures. These predictions contradict the PIT (phase inversion temperature) idea, that below the PIT amphiphile/oil/water systems form only "oil-in-water" emulsions and above the PIT they form only "water-in-oil" emulsions. By using electrical conductivity measurements to determine the emulsion morphologies at different temperatures for systems of constant composition, we show for the system studied that the previous predictions of the dispersion morphology diagram are correct.

Introduction

According to the PIT (phase inversion temperature) idea, below the PIT amphiphile/oil/water systems form O/W ("oil-in-water") emulsions and above the PIT they form W/O ("water-in-oil") emulsions.[1] It has been shown[2] that this belief is consistent with the so-called "Bancroft rule", that in an emulsion the phase of greater surfactant concentration is always the continuous phase.[3-5]

The temperature-dependent phase behavior of nonionic amphiphile/oil/water systems has been determined[6-8] in great detail since the PIT idea was first stated. As a result, it is now known that a "phase inversion temperature" cannot be defined precisely in terms of emulsion behavior, because the idea is intimately connected with the formation of conjugate top, middle, and bottom phases, and these phases form over a range of temperatures.[8] However, the phase inversion temperature can be given a precise definition; for example, it can be identified with the "optimum" temperature, at which the interfacial tension between the top and bottom phases passes through a minimum.[9]

Moreover, detailed knowledge of the temperature-dependent phase behavior of nonionic amphiphile/oil/water systems has made it possible to design experiments to clarify the relationships between phase behavior and emulsion behavior.[10-13] In these experiments, electrical conductivities were measured to determine the emulsion morphologies, and emulsions were always prepared from conjugate (i.e. preequilibrated) phases.[10-13] (For nonmultiple emulsions of two phases, the emulsion morphology is defined by which phase is the continuous phase or, equivalently, which phase is the dispersed one.[14])

On the basis of these measurements and others already in the literature, we constructed a model "dispersion morphology diagram", which predicts the relationships between the morphologies of nonmultiple dispersions and the phase behavior in amphiphile/oil/water temperature diagrams.[11] The dispersion morphology diagram includes all six nonmultiple dispersion

†Adjunct, Institute for Applied Surfactant Research, and School of Chemical Engineering and Materials Science, University of Oklahoma, Norman, OK.

‡Present address: Department of Chemical Engineering, West Virginia University, Morgantown, WV 26506.

(1) Shinoda, K.; Kunieda, H. In *Encyclopedia of Emulsion Technology*; Becher, P., Ed.; Marcel Dekker: New York, 1983; Vol. 1, p 337.
(2) Smith, D. H. In *Microemulsion Systems*; Rosano, H. L., Clausse, M., Eds.; Marcel Dekker: New York, 1987; p 83.
(3) Bancroft, W. D. *J. Phys. chem.* **1913**, *17*, 501. Bancroft's rule is often misquoted to the effect that "the external phase of the emulsion *is* [always] the one that contains most of the surfactant" (italics added); see, e.g., refs 4 and 5. The actual statement was, in effect, that the phase of greater surfactant concentration *tends* to be the continuous phase.
(4) Ross, S.; Morrison, I. D. *Colloidal Systems and Interfaces*; Wiley: New York, 1988; p 269.
(5) Salager, J.-L. In *Encyclopedia of Emulsion Technology*; Becher, P., Ed.; Marcel Dekker: New York, 1988; Vol. 3, p 79.
(6) Kunieda, H. *Bull. Chem. Soc. Jpn.* **1983**, *56*, 625.
(7) Smith, D. H. *J. Colloid Interface Sci.* **1984**, *102*, 435.
(8) Smith, D. H. *J. Colloid Interface Sci.* **1985**, *108*, 471.
(9) Smith, D. H. *AOSTRA J. Res.* **1988**, *4*, 245.
(10) Smith, D. H.; Lim, K.-H. *Proc. Soc. Pet. Eng. Int. Symp. Oilfield Chem., Houston, TX, Feb. 8-10, 1989*; SPE 18496; *Soc. Pet. Eng., Production Eng.* **1990**, *5*, 265.
(11) Smith, D. H.; Lim, K.-H. *J. Phys. Chem.* **1990**, 94, 3746.
(12) Smith, D. H.; Lim, K.-H. *Langmuir* **1990**, *6*, 1071.
(13) Lim, K.-H.; Smith, D. H. *J. Dispersion Sci. Technol.* **1990**, *11*, 529.
(14) Ross, S.; Kornbrekke, R. E. *J. Colloid Interface Sci.* **1981**, *81*, 58.